

PLANT SCIENCES

NPF transporters in synaptic-like vesicles control delivery of iron and copper to seeds

Zhen-Fei Chao^{1,2}, Ya-Ling Wang¹, Yuan-Yuan Chen³, Chu-Ying Zhang^{1,4}, Peng-Yun Wang^{1,4}, Tao Song^{1,2}, Chu-Bin Liu^{1,2}, Qiao-Yan Lv^{1,2}, Mei-Ling Han¹, Shan-Shan Wang¹, Jianbing Yan³, Ming-Guang Lei¹, Dai-Yin Chao^{1*}

Accumulation of iron in seeds is essential for both plant reproduction and human nutrition. Transport of iron to seeds requires the chelator nicotianamine (NA) to prevent its precipitation in the plant vascular tissues. However, how NA is transported to the apoplast for forming metal-NA complexes remains unknown. Here, we report that two members of the nitrate/peptide transporter family, NAET1 and NAET2, function as NA transporters required for translocation of both iron and copper to seeds. We show that NAET1 and NAET2 are predominantly expressed in the shoot and root vascular tissues and mediate secretion of NA out of the cells in resembling the release of neurotransmitters from animal synaptic vesicles. These findings reveal an unusual mechanism of transmembrane transport in plants and uncover a fundamental aspect of plant nutrition that has implications for improving food nutrition and human health.

INTRODUCTION

Two billion people worldwide are affected by iron (Fe) deficiency (1, 2), because most plant-derived staple foods are low in iron and high in anti-nutrition factors that inhibit the bioavailability of Fe (3). Metal homeostasis in plants is dependent on tight coordination of ion transporters, low-molecular mass metal chelators, and membrane transporters for chelators and metal-chelate complexes (4). Nicotianamine (NA) is one of the endogenous metal chelators that are essential for long-distance transport of iron and other metals to sink organs (5, 6). NA is also one of the best enhancers for the absorption of dietary Fe in human and other animals, as it is able to efficiently reverse the impact of anti-nutritional factors (7, 8). Therefore, NA and NA-chelated Fe are very important for both plant and plant-based Fe nutrition.

NA is synthesized from three molecules of S-adenosyl methionine by NICOTIANAMINE SYNTHASEs (NASs). It has an ideal feature for facilitating phloem and/or xylem loading of metals and rhizosphere uptake of Fe (9, 10). YELLOW-STRIFE 1 (YS1) and YSL-LIKE (YSL) proteins belonging to the major facilitator superfamily (MFS) mediate the transport of metal-NA complexes into cells. ZmYS1 was the first characterized Fe(II)-NA transporter that participates in Fe absorbing from soil in maize (11, 12), while YSL1 and YSL3 in *Arabidopsis thaliana* were implicated in the loading of the Fe(II)-NA complex to the phloem during reproductive stage (13, 14). Comparatively, transporters controlling efflux of NA remain unclear. Two MFS transporters OsTOM1 (transporter of mugineic acid 1) and OsTOM2 were reported to function in secretion of the NA analog mugineic acid (2'-deoxymugineic acid) out of rice roots (15). OsENA1 (efflux transporter of NA 1) and OsENA2, two homologs of OsTOM1/2, were found to have NA efflux activity when heterologously expressed in *Xenopus* oocytes (15), but knockout or overexpression of OsENA1/2 did not result in any phenotype related to Fe, questioning their real roles in rice (16). AtZIF1 is an ortholog of OsTOM1/2 in

A. thaliana, but its role was suggested to transport NA or metal-NA complexes into vacuoles (17). Therefore, what transporter mediates the efflux of NA to create a pool of chelated Fe and Cu for uptake into the phloem and/or the xylem for transport to the seed remains a long-sought key question in plant nutrition.

Nitrate transporter 1/peptide transporter (NRT1/PTR) family transporters were found to play essential and diverse roles in material transport and their substrates can be nitrate, oligopeptides, glucosinolates, and phytohormones (18–21). NA is a nonprotein amino acid, which we thought is similar to an oligopeptide in structure. We thus hypothesized that this molecule might be a substrate of some NPF transporters. By using a yeast system, we identified NPF5.8 and NPF5.9 in *A. thaliana* as NA efflux transporters (NAETs), and further genetic and molecular studies established that these two transporters control secretion of NA in xylem and phloem and thus play essential role in translocation of Fe and Cu to the seeds. This study substantially advances our understanding of metal homeostasis in plants with implications to biofortification efforts.

RESULTS

Identification of NAETs in *A. thaliana*

Because of lack of endogenous NAS, *Saccharomyces cerevisiae* (yeast) is unable to synthesize NA and is expected to lack transporters mediating secretion of NA out of the cells. We thus designed a yeast screening system to identify the genes responsible for NA efflux in plants (Fig. 1A). We first introduced an NAS gene *AhNAS3* from *Arabidopsis halleri* into a *S. cerevisiae* (yeast) strain NMY51 to generate a yeast strain (NMY51NA) capable of biosynthesizing NA. We then transformed yeast NMY51NA with 8 genes of the YSL family and 53 genes of the NPF family (Fig. 1, A and B), which we predicted to be candidate transporters mediating NA efflux as NA mimics amino acids or oligopeptides in structure. To identify yeast strains with the capability to secrete NA, we used an immunological dot blot approach with anti-NA antibody. To examine the specificity of the NA antibody we used, we performed a dot blot to detect NA in the leaves of wild-type and a mutant *nas4x-crispr*, in which all four NAS genes were knocked out by the CRISPR-Cas9 technology (fig. S1). Ultraperformance liquid chromatography–mass spectrometry

¹National Key Laboratory of Plant Molecular Genetics, CAS Center for Excellence in Molecular Plant Sciences, Shanghai Institute of Plant Physiology and Ecology, Chinese Academy of Sciences, Shanghai 200032, China. ²University of Chinese Academy of Sciences, Beijing 100049, China. ³National Key Laboratory of Crop Genetic Improvement, Huazhong Agricultural University, Wuhan 430070, China. ⁴School of Life Science, Henan University, Kaifeng 457000, China.

*Corresponding author. Email: dychao@cemaps.ac.cn

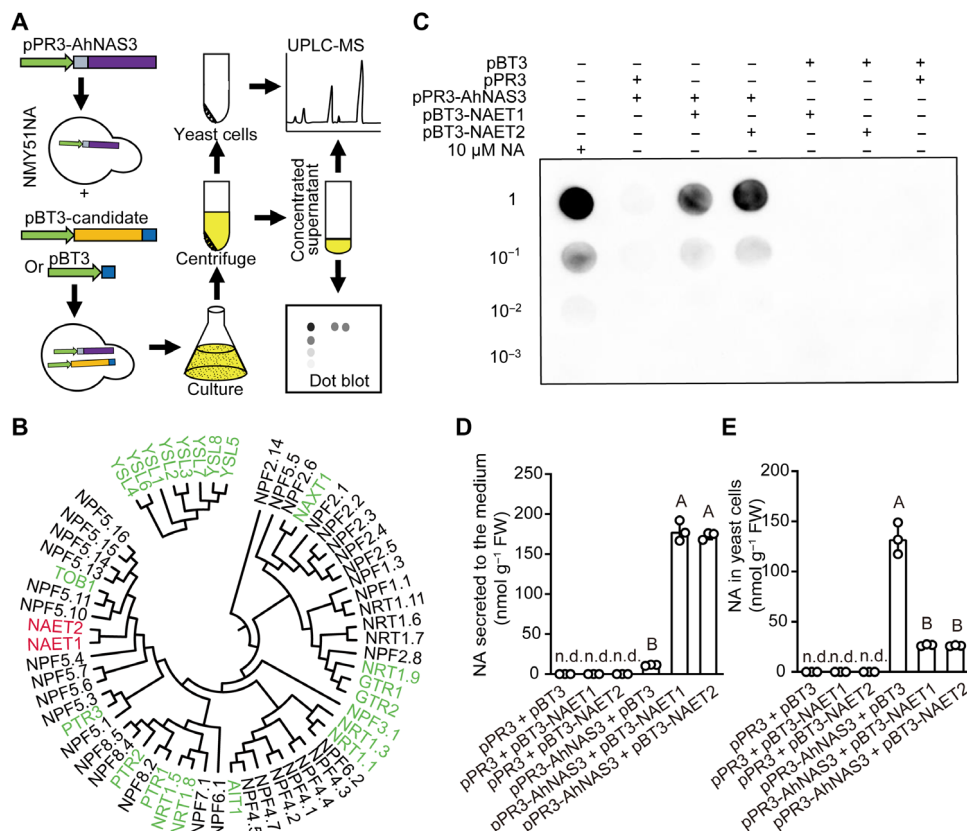


Fig. 1. Identification of NAETs in *Arabidopsis* by using a yeast system. (A) A flowchart of screening for candidate genes encoding NAETs. Green arrows, *Cyc1* promoter; purple bars, *AhNAS3*; orange bars, candidate genes; gray and blue bars, protein tags. (B) Phylogenetic tree of the YSL family and the NPF family in *A. thaliana*. (C) Dot blot using antibody raised against NA shows the secretion of NA into the medium by NAET1 and NAET2. Dilution factors were shown at the left. (D and E) The NA amount in the medium (D) secreted from the yeast cells and the NA amount retained in the cells (E). n.d., not detectable. Error bars represent means \pm SDs ($n = 3$ independent samples). The different letters above the bars indicate significant differences at $P < 0.01$ [one-way analysis of variance (ANOVA)].

(UPLC-MS) analysis showed that NA was not detectable in the *nas4x-crispr* mutant (fig. S1C), and the dot blot produced the same result (fig. S1D), confirming that the NA antibody we used is specific to NA.

The dot blot experiment detected NA in the medium cultivating yeast strains expressing *AhNAS3* and an NPF family member *NPF5.8* (At5g14940) or its close homolog *NPF5.9* (At3g01350), indicating that the two genes encode proteins facilitating efflux of NA out of yeast cells (Fig. 1C and fig. S2). The two proteins share 84% similarity, and the sequences of their orthologs in other plant species are conserved (fig. S3). The NA contents in the growth medium and the yeast cells were quantified using UPLC-MS. Expression of *NPF5.8* or *NPF5.9* in NMY51NA leads to a 15-fold increase in NA secretion to the growth medium (Fig. 1D) and an 80% reduction in the NA associated with the yeast cells (Fig. 1E). However, the presence of *NPF5.8* or *NPF5.9* does not affect the concentration of any other metals, including Fe, either in the medium or yeast cells (fig. S4). This suggests that *NPF5.8* and *NPF5.9* function as NAETs rather than transporters for metal-NA complexes. We then named the two transporters NAET1 and NAET2, respectively.

Phenotypes of *naet1naet2* in development and NA homeostasis

To study the physiological roles of *NAET1* and *NAET2* in *A. thaliana*, we generated two knockout mutants in the Col-0 background for

each of the genes by using CRISPR-Cas9 technology (fig. S5). The two mutants, free of the Cas9 construct after segregation, were named *naet1* and *naet2*, respectively. However, neither *naet1* nor *naet2* exhibits any obviously visible phenotypes (Fig. 2, A to E, and fig. S6, A to C). We then constructed a double-mutant *naet1naet2* by crossing *naet1* and *naet2*. The double-mutant *naet1naet2* exhibits leaf chlorosis and retarded growth (Fig. 2A and fig. S6A). Furthermore, *naet1naet2* has severe defects in embryo development (fig. S6D), leading to termination of development of most seeds (Fig. 2, B and C). Even the seeds of *naet1naet2* that are not terminated at the embryo development stage are abnormal in the shape, color (fig. S6C), and germination rate (Fig. 2, D and E). *NAET1* and *NAET2* are therefore functionally redundant and essential for normal growth and development. The phenotypes of *naet1naet2* are similar to those of the tomato *chloronerva* and *A. thaliana* mutants of *nas4x-2* and *ysl1yls3*, which are unable to synthesize NA or transport metal-NA complexes (5, 13, 22), consistent with the conclusion that *NAET1* and *NAET2* are involved in NA homeostasis.

In addition to the visible phenotypes, we found that the seeds and flowers of the *naet1naet2* double mutant contain 73.6 and 53.7% lower NA levels than wild type, respectively, whereas the NA content in *naet1naet2* roots is sixfold higher (Fig. 2F). These data demonstrate that *NAET1* and *NAET2* control translocation of NA from roots to shoots and/or from shoots to seeds. However, the NA

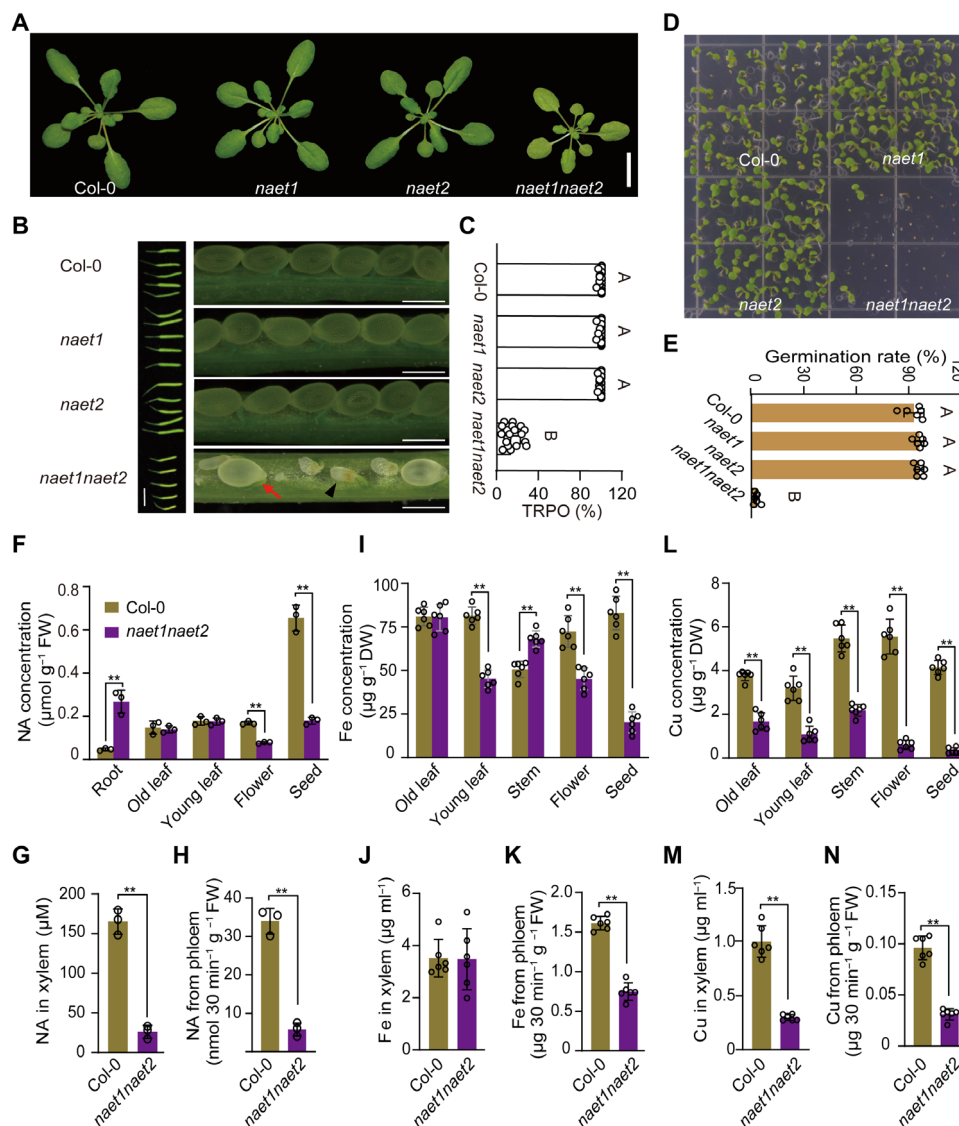


Fig. 2. Phenotypes of the *naet1*, *naet2*, and *naet1naet2* mutants. (A) Representative images of Col-0, *naet1*, *naet2*, and *naet1naet2* grown on soil irrigated with one-fourth Hoagland's for 4 weeks. (B) Siliques (left) and developmental seeds (right) of Col-0 and the mutants. The red arrow indicates a plump ovule, while the black triangle indicates an aborted ovule. (C) The rate of plum ovules (TRPO) in each silique ($n = 19$). (D) Seed germination of different genotypes on one-half MS medium. (E) Quantification of seed germination rates of different genotypes ($n = 6$). (F to N) The NA (F, G, and H), Fe (I, J, and K), and Cu (L, M, and N) concentration in different organs (F, I, and L), xylem saps (G, J, and M), and phloem saps (H, K, and N) of Col-0 and *naet1naet2*. [$n = 6$ (I to N) and 3 (F to H)]. Error bars represent means \pm SDs. Statistical differences were shown in different letters ($P < 0.01$; one-way ANOVA) or $**P < 0.01$; Student's t test. Scale bars, 1 cm [(A) and (B), left] and 500 μm [(B), right].

contents are not affected in the leaves of *naet1naet2* (Fig. 2F). Because leaves are also an important source organ for NA synthesis (6), unchanged NA content in the leaves of *naet1naet2* might reflect a balance between a decreased inflow of NA from roots to leaves and a decreased NA outflow from leaves to flowers and seeds. Consistent with this, the NA contents in both the phloem and xylem saps are markedly reduced in *naet1naet2*, by 84 and 83%, respectively, compared with wild type (Fig. 2, G and H). These data indicate that NAET1 and NAET2 control the cellular efflux of NA necessary for subsequent loading of NA into phloem and xylem.

Ionic phenotype of *naet1naet2*

NA is an effective chelate for Fe transport at the neutral or slightly alkaline pH in the phloem because of its high binding affinity and

stability for Fe(II) compared to other ligands such as organic acids (23). Consistent with this, we found that the Fe content in the seeds of *naet1naet2* is reduced by 75.5% compared with that of wild type (Fig. 2I). As the shortage of iron in the seeds may be causing the defects in embryo development and seeds germination, we sprayed Fe(II)-EDTA on the flowers and siliques of *naet1naet2*. This treatment partially rescued these defects (fig. S6E). These data elucidate that NAET1 and NAET2 are required for Fe delivery to the developing seeds.

In addition to seeds, the translocation of Fe to flowers and young leaves of *naet1naet2* is also notably impaired, albeit to a lesser degree (Fig. 2I). In contrast, the Fe contents in the old leaves and stems are not affected or even slightly increased by knockout of NAET1 and NAET2 (Fig. 2I), indicating that the trafficking of Fe to the sink

organs, but not the source organs, is controlled by NAET1 and NAET2. Consistently, the Fe content in phloem sap collected from the old leaves of *naet1naet2* decreases by 53.6% compared with Col-0, whereas the Fe content in the xylem sap is not affected (Fig. 2, J and K). This is further supported by a reciprocal graft experiment performed between wild type and *naet1naet2*, which showed that the NAET1 and NAET2 in the shoots play a major role in the translocation of Fe to sink organs (Fig. 3A).

In contrast to Fe, the Cu content in the old leaves of *naet1naet2* is decreased by 51.5% (Fig. 2, L and M), indicating that NAET1 and NAET2 are required for Cu translocation from roots to shoots through the xylem. This is consistent with the Cu(II)-NA complex being much more stable than Fe(II)-NA in the acidic xylem sap (23). The larger decrease of Cu accumulation in sink organs of *naet1naet2* (Fig. 2L) suggests that NAETs contribute to transport of Cu in both xylem and phloem. This was supported by the grafting experiment, which shows that the decrease of Cu in the old leaves is totally driven by roots, while the roots and shoots both contribute to the Cu translocation to the seeds and young leaves (Fig. 3B). In addition, the Cu contents are decreased by 65.5% in the xylem sap and by 67.7% in the phloem sap of *naet1naet2* (Fig. 2, M and N), confirming that NAETs are required for both xylem and phloem transport of Cu.

Cobalt (Co) is another essential micronutrient requiring NAET1 and NAET2 for homeostasis. The Co-related phenotypes of *naet1naet2* are very similar to that related to Cu (Fig. 3C and fig. S7, A to C). In contrast, Zn and Ni are not affected in the *naet1naet2* double mutant (fig. S7, D to I), suggesting that NA is not involved in long-distance

transport of Zn and Ni, contrary to what has been proposed (24, 25). The differences between previously proposed hypothesis and our observations may be attributed to the differences in the metal transport strategies or compensation mechanisms between hyperaccumulators and nonhyperaccumulators such as *A. thaliana*.

Expression and subcellular localization of NAET1 and NAET2

Histochemical staining of plants expressing *pNAET1::GUS* or *pNAET2::GUS* reveals that both NAET1 and NAET2 are mainly expressed in the vascular bundles of roots, leaves, and stems, as well as in some leaf epidermal and mesophyll cells to a lesser extent (Fig. 4, A to C, and fig. S8). Cross sections of these tissues show that NAET1 and NAET2 are mainly expressed in the pericycle and the parenchyma cells surrounding the xylem and phloem (Fig. 4, D to F). This localization is consistent with NAET1 and NAET2 driving efflux of NA from cells surrounding the vascular tissue for subsequent loading into the xylem and phloem. In the leaf veins and the stems, NAET1 and NAET2 are preferentially expressed in the parenchyma cells of the phloem rather than of the xylem (Fig. 4, E and F), suggesting that the two genes are more important for phloem transport of NA and metal-NA complexes in the shoot tissues.

We also generated stable transgenic lines expressing *pNAET1::NAET1-GFP* or *pNAET2::NAET2-GFP* in the *naet1naet2* double-mutant background. Phenotyping of the transgenic lines shows that either *pNAET1::NAET1-GFP* or *pNAET2::NAET2-GFP* is able to complement the defects of *naet1naet2* in developmental and ionic phenotypes (fig. S9), indicating that the green fluorescent protein (GFP) tag

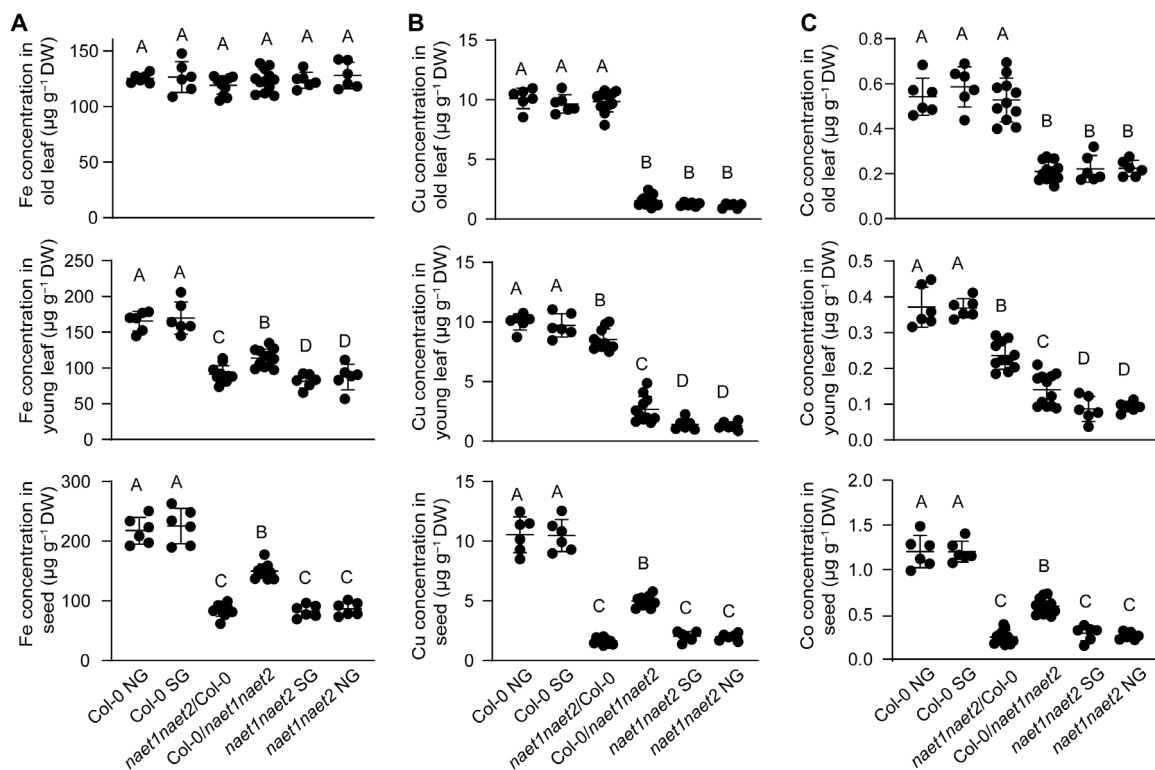


Fig. 3. Ionome changes in different organs of grafted plants between Col-0 and *naet1naet2*. (A to C) Fe (A), Cu (B), and Co (C) concentration in different grafted plants. NG, nongrafted plants; SG, self-grafted plants; *naet1naet2*/Col-0, grafted plants with *naet1naet2* as shoot and Col-0 as root. Col-0/*naet1naet2*, grafted plants with Col-0 as shoot and *naet1naet2* as root. The values are shown as the means \pm SDs ($n = 6$ to 12 independent samples). The different letters indicate significant differences at $P < 0.01$ (one-way ANOVA with Tukey's post hoc test).

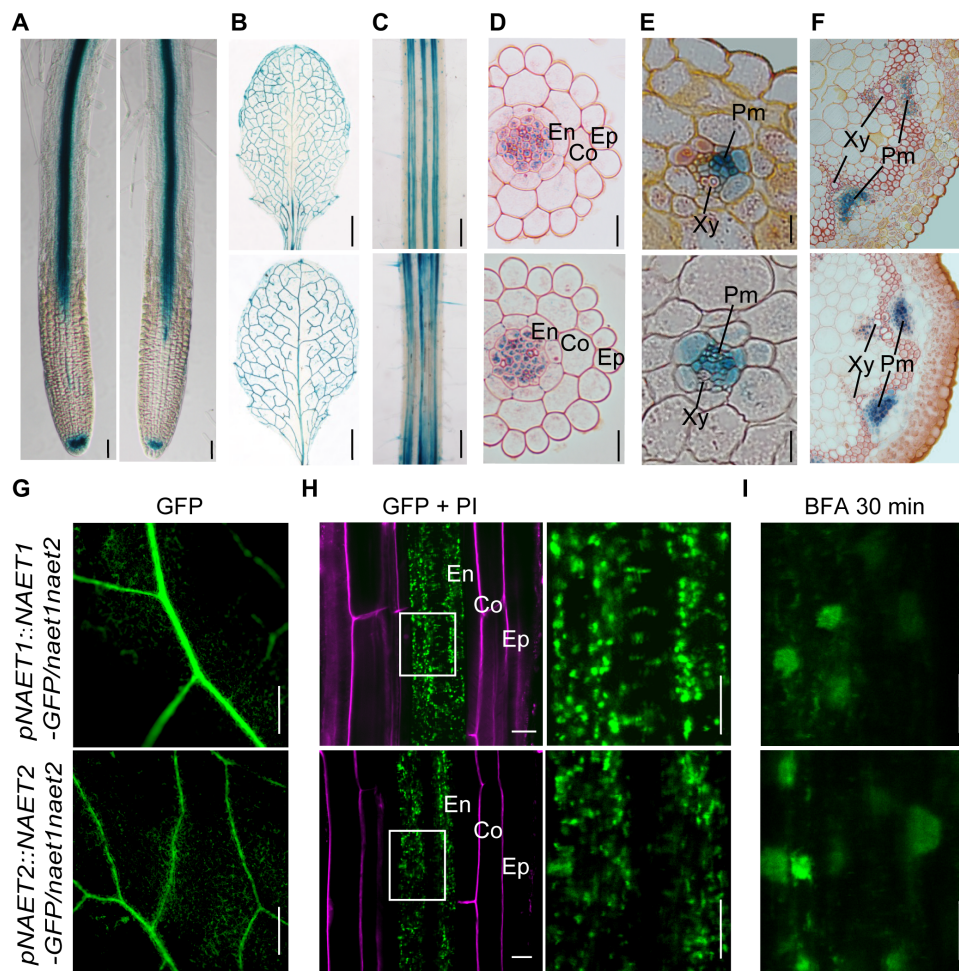


Fig. 4. Expression patterns of NAET1 and NAET2 and subcellular localization of their encoding proteins. (A to C) Representative images of GUS-stained roots (A), leaves (B), and stems (C) expressing *pNAET1::GUS* [(A), left; and (B) to (F), top] and *pNAET2::GUS* [(A), right; and (B) to (F), bottom]. $n = 6$ independent transgenic lines. (D to F) Cross sections of roots (D), leaves (E), and stems (F) in (A) to (C). En, endodermis; Co, cortex; Ep, epidermis; Pm, phloem; and Xy, xylem. (G and H) Representative images of the leaves (G) and the roots (H) of *naet1naet2* expressing *pNAET1::NAET1-GFP* or *pNAET2::NAET2-GFP*. $n = 6$ independent transgenic lines. The right of (H) shows the enlarged pictures in the white rectangles in the left. (I) NAET1-GFP and NAET2-GFP were aggregated to form BFA bodies after the seedlings in (H) were treated with BFA for 30 min. Scale bars, 50 μm [(A), (F), and (G)], 0.25 cm (B), 1 mm (C), and 20 μm [(D), (E), and (H) to (I)].

does not affect the function of NAET1 or NAET2. The fluorescence signals in these lines are consistent with the tissue-specific expression patterns of NAET1 and NAET2 revealed by the promoter-driven β -glucuronidase (GUS) experiment (Fig. 4, G and H). We also observed the subcellular localization of the NAET1-GFP and NAET2-GFP. Unexpectedly, the two proteins are not localized to either the plasma membrane or the tonoplast where other NPF transporters have been found (20, 26). Instead, they appear to be distributed in some vesicle-like structures (Fig. 4H and fig. S10, A and B). These compartments are sensitive to the vesicle trafficking inhibitor brefeldin A (BFA) (Fig. 4I and fig. S10A), indicating that NAET1 and NAET2 are localized in the secretory vesicles.

NA secretion depending on NAETs resembles release of neurotransmitters

In animals, some neurotransmitters are collected into synaptic vesicles by their transporters before being secreted out of the synapses through vesicle trafficking (27, 28). The vesicular localization of NAET1

and NAET2 inspired us to test whether cellular efflux of NA is mediated by a presynaptic vesicle-like mechanism. We found that the intracellular NA is distributed in the vesicle-like compartments in wild type (Fig. 5A), which is consistent with previous observations made using immunoelectron microscopy (17). In contrast, the NA distribution is dispersed evenly in the cytoplasm in the *naet1naet2* double mutant (Fig. 5A), while the fluorescence signal was not detectable in the *nas4x-crispr* mutant (fig. S1E), further confirming the specificity of the NA antibody. Further examination of the NA distribution in the transgenic lines expressing NAET1-GFP or NAET2-GFP revealed that the intracellular NA compartments overlap with the endosomal vesicles where NAET1-GFP and NAET2-GFP are localized (Fig. 5B). These data indicate that NAETs function mainly in collection of NA into the endosomal vesicles, which is subsequently secreted. A 30-min BFA treatment is able to notably suppress unloading of NA into the phloem sap and the xylem sap (Fig. 5, C and D), further supporting the major role of exocytosis rather than plasma membrane transporters in secretion of NA. Of course,

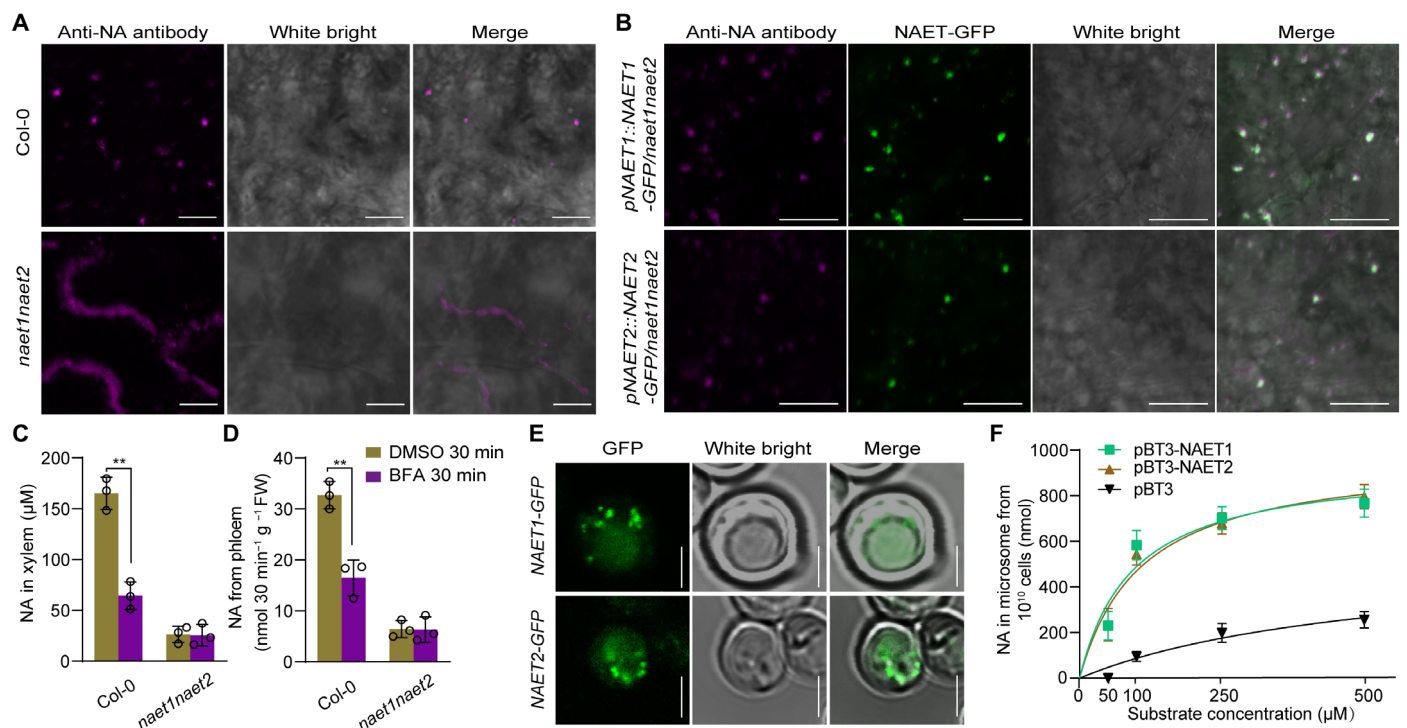


Fig. 5. NAET1 and NAET2 transport NA into synaptic-like vesicles. (A) Intracellular distribution of NA in the leaf epidermal cells of Col-0 and *naet1naet2* revealed by an immunofluorescence assay with the anti-NA antibody. (B) Colocalization of NA with NAET1 and NAET2 in synaptic-like vesicles. Immunostaining with the anti-NA antibody was performed in leaf epidermal cells of the transgenic lines expressing *pNAET1::NAET1-GFP* or *pNAET2::NAET2-GFP*. Images are representative of six independent lines. Fluorescence from the secondary antibody (magenta) and the GFP (green) are shown. (C and D) Effects of a 30-min BFA treatment on NA contents in xylem sap (C) or phloem sap (D) of Col-0 and *naet1naet2*. (E) Subcellular localization of NAET1-GFP and NAET2-GFP in yeast cells. (F) A kinetic analysis of NAET1 and NAET2 in the vesicles isolated from *S. cerevisiae* expressing NAET1 and NAET2. Error bars represent means \pm SDs. $n = 3$ independent samples. $**P < 0.001$ (Student's *t* test). Scale bars, 20 (A) and 10 μm (B).

we do not mean to totally exclude the possibility that transient localization of NAET1 and NAET2 in plasma membrane might also contribute, although very little, to the secretion of NA.

We found that NAET1 and NAET2 expressed in yeast also localize to vesicle-like compartments (Fig. 5E), suggesting that the two transporters mediate efflux of NA from the yeast via the same mechanism as that in plant. By using the microsomal vesicles isolated from the NMY51 strain expressing *NAET1* or *NAET2*, we uncovered that the NAET1 and NAET2 transport NA from the incubation solution to microsomes in a dose-dependent manner (Fig. 5F). The Michaelis constant (K_m) values of NAET1 and NAET2, estimated from the fitted Michaelis-Menten equations, are about 98 and 93 μM , respectively, establishing that both NAET1 and NAET2 are NA transporters in the vesicles.

Combining all the results, we therefore proposed a model that NAETs mediate secretion of NA to regulate metal homeostasis in *A. thaliana* (Fig. 6). In the vascular cells, cytoplasmic NA is first transported into secretory vesicles by two NAET proteins, and then the vesicles release NA through exocytosis to create an apoplastic NA pool. In the root xylem, Cu and Co are complexed by apoplastic NA, and these metal-NA complexes are migrated to the shoot along with the xylem sap flow. In the shoot phloem, the near-neutral pH environment allows formation of metal-NA complexes for Fe, Cu, and Co, and these metal-NA complexes are loaded into sieve tube by YLS1/3 for long-distance transport to sink organs (Fig. 6).

DISCUSSION

The metabolite NA is ubiquitous in the plant kingdom and plays indispensable roles in plant metal homeostasis. Defective in NA synthesis or transport of metal-NA complexes results in a series of defects including leaf chlorosis and decreased fertility (5, 14, 22). Genes involved in NA synthesis and loading metal-NA complexes into phloem have been identified or implicated for a couple of decades (5, 22), but the missing link of the NA-mediated metal homeostasis is that how NA is secreted out of the cells. Identification of NAET1 and NAET2 here addresses this long-sought mystery. This study, together with previous data, established that cytoplasmic NA is first collected into a type of secretory vesicles by NAET1 and NAET2 and is then secreted through exocytosis to the apoplastic space, where NA meets free metal ions or exchanges metals with other metal chelates to form the metal-NA complexes. The metal-NA complexes in the apoplastic space are next transported into phloem by the influx metal-NA transporters.

NA has an ideal structural feature to form stable complexes with metal ions, such as Fe^{2+} , Cu^{2+} , and Co^{2+} , in neutral or near-neutral pH environments like phloem and is thus believed to be almost the exclusive chelator for these metals in the phloem (10, 23). Under low-pH conditions like xylem, Fe(II)-NA tends to be dissociated but Cu(II)-NA is still very stable (23). Therefore, NA is also believed to be required for translocation of Cu through xylem. Consistent with these hypotheses, both Fe and Cu were found to be notably

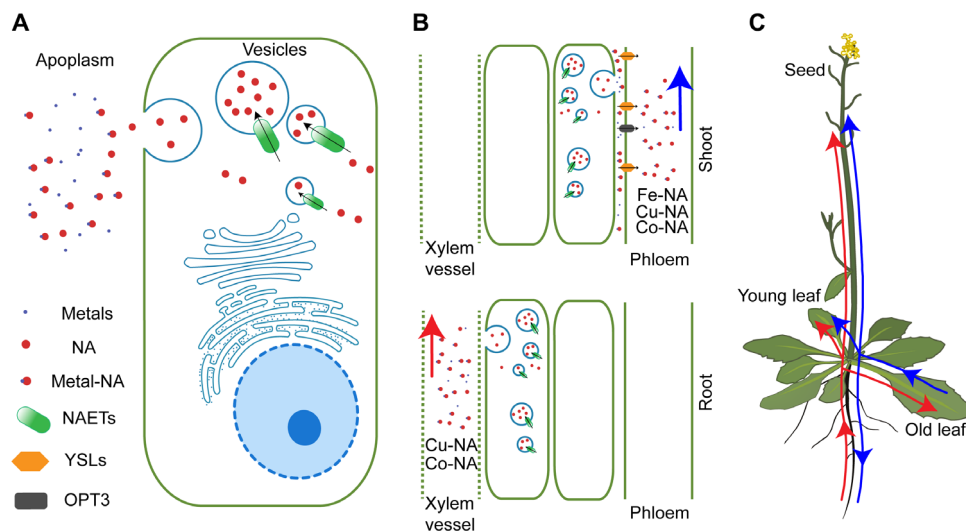


Fig. 6. Proposed functional mechanism of NAET1 and NAET2 in metal homeostasis of *A. thaliana*. (A to C) Functions of NAET1 and NAET2 at cell (A), tissue (B), and organ (C) levels. Cytoplasmic synthesized NA is transported into secretory vesicles by NAET proteins, followed by secretion to the apoplastic space through exocytosis for forming metal-NA complexes. In the root xylem, Cu and Co are complexed by the secreted NA, followed by migration to the shoot along with the xylem flow. The metal-NA complexes for Fe, Cu, and Co are able to be formed in the apoplastic space of the shoot phloem and can be loaded into phloem cells by YLS1/3 for long-distance transport to sink organs. Red arrows indicate the xylem flow and blue arrows indicate the phloem flow. NA, metals, metal-NA complexes, NAETs, YSLs, and OPT3 are shown in the figure as indicated.

decreased in the sink organs of the tomato *chloronerva* (*chl*n) mutant, but only Cu rather than Fe is decreased in the old leaves of *chloronerva* (29, 30). The *A. thaliana* NA synthesis mutant *nas4x-2* is also impaired in Fe translocation to sink organs, but the Cu content was not found to be affected in *nas4x-2* (5, 6), probably reflecting complexity of metal homeostasis. YSL1 and YSL3 in *A. thaliana* were proposed to translocate metal-NA complex into phloem parenchyma cells (13). The double-mutant *ysl1ysl3* displays interveinal chlorosis and has decreased fertility, similar to *chl*n and *nas4x-2*. The ion phenotype of *ysl1ysl3* is more similar to *chl*n rather than *nas4x-2*, as *ysl1ysl3* accumulates notably less Fe and Cu in sink organs (13, 14). The *naet1naet2* double mutant exhibits an excellent phenocopy of *ysl1ysl3* in sink organ ions, probably because YSLs are very likely to literally pick up metal-NA in the phloem where the NAETs leave off NA. However, a difference between *ysl1ysl3* and *naet1naet2* is that the latter accumulates notably lower Cu in the aged leaves, while the former accumulates higher (31). This can be explained that YSLs only control metal-NA uptake in the phloem, while NAETs control NA release in both phloem and xylem. In addition, AtOPT3 and BdYSL3 were reported to mediate free metal ions transport in vitro and mediate ion loading into the phloem companion cells and delivery to seeds (32, 33), reflecting the flexibility and complexity of metal transport.

NAET1 and NAET2 are two members of the NPF family (34), which belongs to an important part of the MFS. In animals, NPF members were first identified as oligopeptide transporter (PTR) proteins involved in the uptake of di- and tri-peptides (35). Their homologs in plants were initially characterized as nitrate or peptide transporters (18). However, in recent years, some other substrates of them were also found, namely, glucosinolates, auxin, abscisic acid, jasmonates, and gibberellins (20, 21, 26, 36, 37). Here, we identified NA as a previous unidentified substrate of the NPF family. Previously, transporters mediating NA secretion in the vascular tissues were most considered to be TOM1/ENA1-like proteins or YSL family members

(11, 15), but our study demonstrated that it is not the case. During evolution, flexibility within the NPF family might allow the transport of these small-molecule substrates sharing structure similarities (21). Given that NA shares similarity with small peptides, it is expected that NA transporters were evolved from the peptide transporters.

All the transporters characterized and described previously in NPF family are, or are thought to be, plasma membrane localized or tonoplast localized (18, 26, 38). However, NAET1 and NAET2 are localized to the secretory vesicles. This localization revealed a previous unknown mechanism for small-molecule secretion in plants. This secretory transport mechanism is previous unidentified in plants and is similar to neurotransmitter exocytosis through synaptic vesicles in animals (27, 39). Structural analysis of these proteins in the future should help understand the molecular basis of the selectivity and the subcellular localization of these two transporters.

Overall, the identification of two NPF/PTR family proteins as NAETs addresses a fundamental question in plant nutrition unresolved for a long time regarding how the essential metal chelator is unloaded to the phloem and xylem for the long-distance transport of iron and copper and highlights the importance of NA and its transporters in plant nutrition. The NPF family transporters have been found to play essential and diverse roles in all major kingdoms of life (18, 20, 35). This finding uncovers a previous unidentified role of the NPF family transporters and provides potential targets for biofortifying crops with enhanced Fe content for human nutrition. We have also found a transport mechanism in plant resembling neurotransmitter release in animal. We suggest that a similar mechanism using synaptic-like vesicles may be used for the delivery of other substances in plants.

MATERIALS AND METHODS

Plant material and growth conditions

The plants used for elemental analysis were grown in a climate-controlled room with growth conditions as previously described (40). The

plants were bottom watered twice a week with modified 0.25× Hoagland's Type II with 10 μM Fe-HBED [N,N'-bis(2-hydroxyphenyl) ethylenediamine-N,N'-diacetic acid] (40). To obtain viable seeds from *naet1naet2*, 150 μM Fe-HBED and 10 μM CuCl₂ and 10 μM CoCl₂ were sprayed to the flowers and siliques when the plants were flowering.

For hydroponic culture, seeds of *A. thaliana* (Col-0 and *naet1naet2*) were stratified for 3 days at 4°C in water and then put on a pipe cover with a pore in the middle of a 1.5-ml Eppendorf tube containing Hoagland solution for 14 days in a chamber at 22°C, 70% relative humidity, and light intensity of 80 μmol m⁻² s⁻¹ on 8-hour light/16-hour dark, as previously described (40). The seedlings together with caps were then transferred to a new box containing Hoagland solution for growing five additional weeks. The medium was refreshed every 4 days.

Vector construction

To generate the mutants of *naet1* and *naet2*, single guide RNAs (sgRNAs) targeting *NAET1* (GCTGGAGGAGAGAAAAGAAG) and *NAET2* (GATTTAGAACAGAAGACAAG) were inserted into the binary vector pHEE401 according to the method as described previously (41). To generate the mutant of *nas4x-crispr*, sgRNAs targeting *NAS1* (CTCACATCCATCGTATTGGC), *NAS2* (ATGTCCCGACCAAAGTCGCC), *NAS3* (GGTTGCCAAGACGAACAAT), and *NAS4* (TAAAGCCTTGTGAAGATGTC) were designed and inserted into the same vector pHEE401. To construct the expression vectors *pNAET1::NAET1-GFP* and *pNAET2::NAET2-GFP*, a 5.1-kb genomic DNA fragment of *NAET1* and a 4.8-kb genomic DNA fragment of *NAET2* (each fragment includes a 2-kb promoter and gene body with stop codon removed) were amplified from Col-0 genomic DNA using the primers NAETs-GFP-F/NAETs-GFP-OV-R. The GFP fragment was amplified using the primers GFP-NAETs-OV-F/GFP-R. Thereafter, each genomic fragment and the GFP fragment were fused by overlapping polymerase chain reaction (PCR) with the primers NAETs-GFP-F and GFP-R. Each fused fragment was inserted into the cloning site between Hind III and Pst I of the binary expression vector *pHMS* (42) by using the Hieff Clone One Step PCR Cloning Kit (Yisheng Co. Ltd., Shanghai, China).

To construct the *pNAET1::GUS* and *pNAET2::GUS* vector, the *NAET1* and *NAET2* promoters were amplified from Col-0 genomic DNA by using primer pairs of *NAET1-GUSF/NAET1-GUSR* and *NAET2-GUSF/NAET2-GUSR*. The fragments were inserted into the cloning site between Hind III and Sal I of the binary vector pCambia1303 to drive *uidA* expression. To construct the transient expression vectors of *pA7-NAET1-GFP* and *pA7-NAET2-GFP*, the coding regions of *NAET1* and *NAET2* were amplified by primer pairs of *NAET1-Xho I/NAET1-Sal I*, and *NAET2-Xho I/NAET2-Sal I*, respectively. The fragments were cloned into the 5' cloning site between Xho I and Sal I of the vector *pA7-GFP*. To construct the transient expression vectors of *pA7-GFP-NAET1* and *pA7-GFP-NAET2*, the coding regions of *NAET1* and *NAET2* were amplified by primer pairs of *NAET1-Xba I/NAET1-Bam HI* and *NAET2-Xba I/NAET2-Bam HI*, respectively, and the fragments were cloned into the 3' cloning site between Xba I and Bam HI of the vector *pA7-GFP*.

For construction of the yeast expression vector *pPR3-AhNAS3*, the coding region of *AhNAS3* was amplified from *A. halleri* complementary DNA (cDNA) by using the primers *AhNAS3-F* and *AhNAS3-R*. The amplified fragment was cloned into the cloning site between Eco RI and Bam HI of the yeast expression vector *pPR3-N*. For

construction of the *pBT3* candidates, the coding region of each gene was amplified from Col-0 cDNA using the primers as listed in data file S2. Each of the fragments amplified was inserted into the cloning site between Hind III and Pst I of the yeast expression vector *pBT3-STE*. To construct the vectors of *pYES2-NAET1-GFP* and *pYES2-NAET2-GFP*, the fragments of *NAET1-GFP* and *NAET2-GFP* were amplified from the vectors of *pA7-NAET1-GFP* and *pA7-NAET2-GFP* by using primers *pYES2-NAETs-F* and *pYES2-GFP-R*, and the fragments were cloned into the cloning site between Hind III and Xba I of the vector *pYES2*. All the primers used were listed in data file S2.

Phylogeny

Protein sequences for plant NPF and YSL family members were retrieved from the public plant genome database Gramene (www.gramene.org). Phylogenetic relationships were inferred using the neighbor-joining method and was computed using the Poisson correction method. Phylogenetic analyses were conducted using the Molecular Evolutionary Genetics Analysis X software (www.megasoftware.net).

A. thaliana grafting

Reciprocal grafting was performed as described previously (43). After the graft unions were established, the grafted plants were examined under a stereoscopic microscope before being transferred into soil to observe the formation of any adventitious roots from the graft unions or above. Fine grafted plants were transferred to potting mix soil and grown in the controlled environment described above. The leaf, flower, and seeds were harvested for elemental analysis after the plants were grown in soil for 4, 8, and 10 weeks, respectively. When being harvested, the plants were examined again to exclude those with adventitious roots or without a clear graft union from the subsequent analysis.

Collection of xylem sap and phloem exudates

For collection of xylem sap, plants were grown in hydroponic culture for 7 weeks. After all rosette leaves were removed, the inflorescence stems were cut using a sharp razor, and xylem sap was collected within 4 hours as described (44). BFA is a vesicle trafficking inhibitor and inhibits the function of adenosine 5'-diphosphate-ribosylation factor guanosine triphosphatases by interacting with their associated guanine nucleotide exchange factors and thereby results in membranous aggregates known as BFA compartments (45). For BFA-treated plants, xylem sap was collected within 30 min.

Phloem exudates were collected by using the EDTA-facilitated method as previously described with some modifications (46). Briefly, whole rosettes of 5-week-old plants grown in artificial soil were removed from the root using a sharp razor and immersed in deionized water before individual leaves were detached at the petiole. Four (eight for the BFA treatment experiment) leaves (the ninth and 10th) collected from two plants (four plants for BFA treatment experiment) were pooled together with the petioles put in a 1.5-ml tube filled with deionized water. The samples were then put in a box covered with cling film to keep a high humidity and incubated in an illuminated growth chamber for 15 min to flash of xylem sap. The petioles were then recut under 5 mM Na₂-EDTA (pH 7.5) under low light and were placed in 250 μl of 5 mM Na₂-EDTA (pH 7.5) for incubation in darkness for 1 hour (30 min for the BFA treatment experiment) in a high-humidity box.

Elemental analysis

The elemental analysis was conducted by inductively coupled plasma MS (ICP-MS) as previously described (47). The plant samples were rinsed with 18.2-megohm Milli-Q Direct Water (Merck Millipore) for four times, and the yeast samples were first rinsed with 1 mM EDTA followed by rinsing with 18.2-megohm Milli-Q Direct Water for four times. Then, the rinsed samples were placed into Pyrex test tubes (16 × 100 mm) to dry in an oven at 65°C for 24 hours. After weighing 12 samples (these weights were used to calculate the weights of rest of the samples), the trace metal-grade nitric acid Primar Plus (Fisher Chemical) spiked with indium internal standard was added to the tubes (1 ml per tube). The samples were then digested in a block heater (DigiPREP MS, Seignior Chemical Products (SCP) Science, QMX Laboratories, Essex, UK) at 115°C for 4 hours. The digested samples were diluted to 10 ml with 18.2-megohm Milli-Q Direct Water (Merck Millipore). The liquid samples including xylem sap, phloem sap, and yeast secrets in the water were diluted with 1.7 ml of 5% HNO₃ for subsequent detection. Elemental analysis was performed using an ICP-MS (NexION 350D, PerkinElmer, USA) coupled with an Apex desolvation system and an SC-4 DX autosampler (Elemental Scientific Inc., USA). Twenty elements (Li, B, Na, Mg, P, S, K, Ca, Mn, Fe, Co, Ni, Cu, Zn, As, Se, Rb, Sr, Mo, and Cd) were monitored. All the solid samples were normalized with a heuristic algorithm using the best measured elements as previously described (40). Further data processing was performed using Microsoft Excel spreadsheet.

Detection of NA

Extraction and qualification of NA from plant and yeast samples follows the procedures as previously described (48). Briefly, ~100 mg of fresh samples was ground in liquid nitrogen and extracted with 300 µl of ultrapure water at 80°C with shaking for 30 min, followed by 20-min centrifugation (13,400g) at 4°C. The supernatant solution was transferred to centrifuge tubes with filters (0.22 µm) and further centrifuged for 10 min at 13,400g. The filtered supernatant solution was determined in an UPLC-MS (QTRAP 6500+, AB SCIEX) using a Thermo Hypercarb C18 column (150 mm by 2.1 mm, 5 µm; Thermo Fisher Scientific, USA) with an amino acid analysis kit. Solvents were water (A) and acetonitrile (B), both acidified with 0.1% (v/v) formic acid. The NA contents in liquid samples including xylem sap, phloem sap, and yeast culture solution were measured with the same procedure except sample grinding. Chemically synthesized NA (Cayman Chemical, USA) was used as a standard.

For detection of NA by dot blot, custom affinity-purified polyclonal anti-NA antibodies were produced by Youke Biotechnology Co. Ltd. (Shanghai, China). More than 5 mg of keyhole limpet hemocyanin-coupled NA was used to immune two rabbits for four times, and the antiserum was purified by bovine serum albumin (BSA)-coupled NA. For dot blot, 2 µl of each sample was spotted on Nytran nylon membrane (0.45 µm) and allowed to dry for 5 min. A mixed amino acid standard (Sigma-Aldrich, USA) was used as negative control. The membrane was then blocked in TBST buffer [50 mM tris-Cl (pH 7.6), 150 mM NaCl, and 0.5% Tween 20] with 5% (w/v) milk at room temperature for 2 hours. Following that the membrane was washed three times with TBST buffer and incubated with anti-NA antibody in TBST overnight at 4°C. The membrane was then washed three times again with TBST and incubated with goat anti-rabbit immunoglobulin G-horseradish peroxidase (HRP) (Abmart Co. Ltd., Shanghai) at room temperature for 1 hour. Next,

the membrane was washed three times again, followed by incubation with the Immobilon Western Chemiluminescent HRP Substrate (Millipore). The blot signals were examined by the Tanon 5200 Chemiluminescent Imaging System (Tanon Co. Ltd., China).

Immunostaining of NA

Immunostaining of NA was performed following the method described previously (49), with modifications. In brief, 7-day-old seedlings were fixed in fixation buffer [4% formaldehyde, 0.02 Triton X-100, 5% dimethyl sulfoxide (DMSO), 60 mM Pipes, 25 mM Hepes, 10 mM EGTA, and 2 mM MgCl₂ (pH 6.9)] for 1 hour and then washed three times with 5% DMSO in PHEM buffer [60 mM Pipes, 25 mM Hepes, 10 mM EGTA, and 2 mM MgCl₂ (pH 6.9)]. Subsequently, the seedlings were digested in 1% cellulose and 0.3% pectinase at 37°C for 30 min to remove cell walls, followed by washing with PHEM buffer. The seedlings were then put into PHEM buffer with 1% Triton X-100, 5% DMSO, and 3% BSA (w/v) at 37°C for 30 min. After washing again with PHEM buffer, the seedlings were put into phosphate-buffered saline (PBS) buffer [10 mM Na₂HPO₄, 1.8 mM KH₂PO₄, 2.7 mM KCl, and 137 mM NaCl (pH 7.4)] with 1:500 diluted anti-NA antibody (Abmart Co. Ltd., Shanghai) and incubated overnight at 4°C. Then, the seedlings were washed for five times with PBS buffer and incubated with the secondary antibody (Transgene, China), which was diluted 1:500 in PBS buffer for 1 hour at 37°C. After washing four times in PBS buffer, the seedlings were then observed using a confocal laser scanning microscope (TCS SP8 STED 3X, Leica).

Cell imaging

The cellular fluorescence was all observed under the Leica TCS SP8 confocal laser scanning microscope. To observe the GFP signals, an excitation wavelength of 488 nm from an argon laser was used, and the emission signal was detected at 500 to 550 nm. For immunostaining of NA, the secondary antibody labeled with Alexa Fluor 405 (Abmart Co. Ltd., Shanghai) was stimulated by 405-nm argon laser and observed at 421 to 450 nm. For propidium iodide fluorescence, the fluorescence excitation and emission wavelengths were 561 and 610 to 630 nm, respectively.

GUS histochemical staining was performed as previously described (50). Pictures were taken for the tissues with GUS signals under a stereo microscope (SMZ1500, Nikon, Japan) or a differential interference contrast (DIC) microscope (ECLIPSE Ni, Nikon, Japan). The ovules were observed under the stereo microscope, and the embryos were observed under the DIC microscope after cleared in chloral hydrate/glycerol/water (8:1:3) mixture for 2 days. The mature seeds of Col-0 and the mutants were also observed under a scanning electron microscope (Merlin Compact, Zeiss, Germany).

Chemical treatment

To observe the effect of BFA treatment on subcellular localization of NAET1 and NAET2, 7-day-old *Arabidopsis* seedlings were cultured with 50 µM BFA for 30 min and then subjected to observation under a confocal laser scanning microscopy (Leica TCS SP8). To examine the effect of BFA treatment on NA secretion into xylem, 7-week-old plants grown in hydroponics were transferred to a new box with 50 µM BFA in hydroponic culture solution, the stems were then immediately cut, and xylem sap was collected within 30 min. To examine the effect of BFA treatment on NA secretion into phloem, the leaves were infiltrated with 50 µM BFA or control solution (0.1% DMSO) just before collection of the phloem sap.

Plant and yeast transformation

For stable transformation of *Arabidopsis* plants, binary vectors were first transformed into the *Agrobacterium tumefaciens* strain GV3101 and then introduced plants using the floral dip method (51). For transient expression of genes in *Arabidopsis* protoplasts, vectors were transferred into protoplasts of Col-0 following methods as described previously (52). For transient expression of genes in *Nicotiana benthamiana* leaf epidermal cells, the expression vectors were first transformed into GV3101, and then leaves of 4-week-old plants were infiltrated with corresponding strains. At 36 hours of injection, signal was observed under a confocal laser scanning microscopy (Leica TCS SP8). Yeast transformation was performed by using the lithium acetate transformation procedure, as described in the *Yeast Protocols Handbook* (Clontech).

Transport activity analysis

The transport activities of NAET1 and NAET2 were examined by using microsomes isolated from yeast strain NMY51 expressing *pYES2-NAET1* or *pYES2-NAET2*. In brief, yeast cells in the exponential growth phase were collected by centrifugation and digested with lyticase (1000 U/g fresh weight cells; Yeasen Biotechnology), and then microsomal vesicles were isolated as described previously (53). To perform the transport activities, the microsomes obtained were resuspended in transport buffer [3 mM adenosine 5'-triphosphate, 5 mM MgCl₂, 10 mM creatine phosphate, creatine kinase (16 U/ml), BSA (1 mg/ml), 100 mM KCl, and 25 mM tris-MES (pH 7.4)] at room temperature. Different concentrations of NA were added in the microsomes, and the mixes were incubated for a time as indicated in the main text at 25°C. After the incubation was ended, each reaction was immediately transferred to an ultracentrifuge tubes with ice-cold washing buffer [100 mM KCl and 25 mM tris-MES (pH 7.4)] and centrifuged at 4°C for 1 hour in 100,000g. The microsome pellet was washed two more times in the same condition before NA analysis.

SUPPLEMENTARY MATERIALS

Supplementary material for this article is available at <https://science.org/doi/10.1126/sciadv.abh2450>

[View/request a protocol for this paper from Bio-protocol.](#)

REFERENCES AND NOTES

- World Health Organization, The World Health report 2002. *Midwifery* **19**, 72–73 (2003).
- E. McLean, M. Cogswell, I. Egli, D. Wojdyla, B. de Benoist, Worldwide prevalence of anaemia, WHO vitamin and mineral nutrition information system, 1993–2005. *Public Health Nutr.* **12**, 444–454 (2009).
- R. Hurrell, I. Egli, Iron bioavailability and dietary reference values. *Am. J. Clin. Nutr.* **91**, 1461S–1467S (2010).
- S. Clemens, Metal ligands in micronutrient acquisition and homeostasis. *Plant Cell Environ.* **42**, 2902–2912 (2019).
- M. Schuler, R. Rellán-Álvarez, C. Fink-Straube, J. Abadía, P. Bauer, Nicotianamine functions in the phloem-based transport of iron to sink organs, in pollen development and pollen tube growth in *Arabidopsis*. *Plant Cell* **24**, 2380–2400 (2012).
- M. Klatte, M. Schuler, M. Wirtz, C. Fink-Straube, R. Hell, P. Bauer, The analysis of *Arabidopsis* nicotianamine synthase mutants reveals functions for nicotianamine in seed iron loading and iron deficiency responses. *Plant Physiol.* **150**, 257–271 (2009).
- L. Zheng, Z. Cheng, C. Ai, X. Jiang, X. Bei, Y. Zheng, R. P. Glahn, R. M. Welch, D. D. Miller, X. G. Lei, H. Shou, Nicotianamine, a novel enhancer of rice iron bioavailability to humans. *PLoS ONE* **5**, e10190 (2010).
- T. Eagling, A. A. Wawer, P. R. Shewry, F.-J. Zhao, S. J. Fairweather-Tait, Iron bioavailability in two commercial cultivars of wheat: Comparison between wholegrain and white flour and the effects of nicotianamine and 2'-deoxymugineic acid on iron uptake into Caco-2 cells. *J. Agr. Food Chem.* **62**, 10320–10325 (2014).
- C. Curie, G. Cassin, D. Couch, F. Divol, K. Higuchi, M. Le Jean, J. Misson, A. Schikora, P. Czernic, S. Mari, Metal movement within the plant: Contribution of nicotianamine and yellow stripe 1-like transporters. *Ann. Bot.* **103**, 1–11 (2009).
- U. W. Stephan, I. Schmidke, V. W. Stephan, G. Scholz, The nicotianamine molecule is made-to-measure for complexation of metal micronutrients in plants. *Biomol.* **9**, 84–90 (1996).
- C. Curie, Z. Panaviene, C. Loulergue, S. L. Dellaporta, J. F. Briat, E. L. Walker, Maize yellow stripe1 encodes a membrane protein directly involved in Fe(III) uptake. *Nature* **409**, 346–349 (2001).
- G. Schaaf, U. Ludewig, B. E. Erenoglu, S. Mori, T. Kitahara, N. von Wirén, ZmYS1 functions as a proton-coupled symporter for phytosiderophore- and nicotianamine-chelated metals. *J. Biol. Chem.* **279**, 9091–9096 (2004).
- B. M. Waters, H. H. Chu, R. J. DiDonato, L. A. Roberts, R. B. Easley, B. Lahner, D. E. Salt, E. L. Walker, Mutations in *Arabidopsis* *Yellow Stripe-Like1* and *Yellow Stripe-Like3* reveal their roles in metal ion homeostasis and loading of metal ions in seeds. *Plant Physiol.* **141**, 1446–1458 (2006).
- H. H. Chu, J. Chiecko, T. Punshon, A. Lanzirotti, B. Lahner, D. E. Salt, E. L. Walker, Successful reproduction requires the function of *Arabidopsis* *YELLOW STRIPE-LIKE1* and *YELLOW STRIPE-LIKE3* metal-nicotianamine transporters in both vegetative and reproductive structures. *Plant Physiol.* **154**, 197–210 (2010).
- T. Nozoye, S. Nagasaka, T. Kobayashi, M. Takahashi, Y. Sato, Y. Sato, N. Uozumi, H. Nakanishi, N. K. Nishizawa, Phytosiderophore efflux transporters are crucial for iron acquisition in graminaceous plants. *J. Biol. Chem.* **286**, 5446–5454 (2011).
- T. Nozoye, N. von Wirén, Y. Sato, T. Higashiyama, H. Nakanishi, N. K. Nishizawa, Characterization of the nicotianamine exporter ENA1 in rice. *Front. Plant Sci.* **10**, 502 (2019).
- M. J. Haydon, M. Kawachi, M. Wirtz, S. Hillmer, R. Hell, U. Krämer, Vacuolar nicotianamine has critical and distinct roles under iron deficiency and for zinc sequestration in *Arabidopsis*. *Plant Cell* **24**, 724–737 (2012).
- Y. F. Tsay, J. I. Schroeder, K. A. Feldmann, N. M. Crawford, The herbicide sensitivity gene *CHL1* of *Arabidopsis* encodes a nitrate-inducible nitrate transporter. *Cell* **72**, 705–713 (1993).
- D. Dietrich, U. Hammes, K. Thor, M. Suter-Grotemeyer, R. Flückiger, A. J. Slusarenko, J. M. Ward, D. Rentsch, AtPTR1, a plasma membrane peptide transporter expressed during seed germination and in vascular tissue of *Arabidopsis*. *Plant J.* **40**, 488–499 (2004).
- H. H. Nour-Eldin, T. G. Andersen, M. Burrow, S. R. Madsen, M. E. Jørgensen, C. E. Olsen, I. Dreyer, R. Hedrich, D. Geiger, B. A. Halkier, NRT/PTR transporters are essential for translocation of glucosinolate defence compounds to seeds. *Nature* **488**, 531–534 (2012).
- C. Corratgé-Faillie, B. Lacombe, Substrate (un)specificity of *Arabidopsis* NRT1/PTR FAMILY (NPF) proteins. *J. Exp. Bot.* **68**, 3107–3113 (2017).
- H.-Q. Ling, G. Koch, H. Bäumlein, M. W. Ganai, Map-based cloning of *chloronerva*, a gene involved in iron uptake of higher plants encoding nicotianamine synthase. *Proc. Natl. Acad. Sci. U.S.A.* **96**, 7098–7103 (1999).
- N. von Wirén, S. Klair, S. Bansal, J.-F. Briat, H. Khodr, T. Shioiri, R. A. Leigh, R. C. Hider, Nicotianamine chelates both Fe^{III} and Fe^{II}. Implications for metal transport in plants. *Plant Physiol.* **119**, 1107–1114 (1999).
- J.-Y. Cornu, U. Deinlein, S. Höreth, M. Braun, H. Schmidt, M. Weber, D. P. Persson, S. Husted, J. K. Schjoerring, S. Clemens, Contrasting effects of nicotianamine synthase knockdown on zinc and nickel tolerance and accumulation in the zinc/cadmium hyperaccumulator *Arabidopsis halleri*. *New Phytol.* **206**, 738–750 (2015).
- U. Deinlein, M. Weber, H. Schmidt, S. Rensch, A. Trampczynska, T. H. Hansen, S. Husted, J. K. Schjoerring, I. N. Talke, U. Krämer, S. Clemens, Elevated nicotianamine levels in *Arabidopsis halleri* roots play a key role in zinc hyperaccumulation. *Plant Cell* **24**, 708–723 (2012).
- M. Michniewicz, C.-H. Ho, T. A. Enders, E. Floro, S. Damodaran, L. K. Gunther, S. K. Powers, E. M. Frick, C. N. Topp, W. B. Frommer, L. C. Strader, Transporter of IBA1 links auxin and cytokinin to influence root architecture. *Dev. Cell* **50**, 599–609.e4 (2019).
- T. C. Sudhof, The synaptic vesicle cycle. *Annu. Rev. Neurosci.* **27**, 509–547 (2004).
- L. E. Eiden, The vesicular neurotransmitter transporters: Current perspectives and future prospects. *FASEB J.* **14**, 2396–2400 (2000).
- A. Pich, G. Scholz, U. W. Stephan, Iron-dependent changes of heavy metals, nicotianamine, and citrate in different plant organs and in the xylem exudate of two tomato genotypes. Nicotianamine as possible copper translocator. *Plant Soil* **165**, 189–196 (1994).
- A. Pich, G. Scholz, Translocation of copper and other micronutrients in tomato plants (*Lycopersicon esculentum* Mill): Nicotianamine-stimulated copper transport in the xylem. *J. Exp. Bot.* **47**, 41–47 (1996).
- B. M. Waters, M. A. Grusak, Whole-plant mineral partitioning throughout the life cycle in *Arabidopsis thaliana* ecotypes Columbia, Landsberg *erecta*, Cape Verde Islands, and the mutant line *ysl1ysl3*. *New Phytol.* **177**, 389–405 (2008).

32. Z. Zhai, S. R. Gayomba, H. I. Jung, N. K. Vimalakumari, M. Piñeros, E. Craft, M. A. Rutzke, J. Danku, B. Lahner, T. Punshon, M. L. Guerinot, D. E. Salt, L. V. Kochian, O. K. Vatamaniuk, OPT3 is a phloem-specific iron transporter that is essential for systemic iron signaling and redistribution of iron and cadmium in *Arabidopsis*. *Plant Cell* **26**, 2249–2264 (2014).
33. H. Sheng, Y. Jiang, M. Rahmati, J.-C. Chia, T. Dokuchayeva, Y. Kavulych, T.-O. Zavodna, P. N. Mendoza, R. Huang, L. M. Smieshka, J. Miller, A. R. Woll, O. I. Terek, N. D. Romanyuk, M. Piñeros, Y. Zhou, O. K. Vatamaniuk, YSL3-mediated copper distribution is required for fertility, seed size and protein accumulation in *Brachypodium*. *Plant Physiol.* **186**, 655–676 (2021).
34. S. Lérán, K. Varala, J.-C. Boyer, M. Chiurazzi, N. Crawford, F. Daniel-Vedele, L. David, R. Dickstein, E. Fernandez, B. Forde, W. Gassmann, D. Geiger, A. Gojon, J.-M. Gong, B. A. Halkier, J. M. Harris, R. Hedrich, A. M. Limami, D. Rentsch, M. Seo, Y.-F. Tsay, M. Zhang, G. Coruzzi, B. Lacombe, A unified nomenclature of nitrate transporter 1/peptide transporter family members in plants. *Trends Plant Sci.* **19**, 5–9 (2014).
35. Y. J. Fei, Y. Kanai, S. Nussberger, V. Ganapathy, F. H. Leibach, M. F. Romero, S. K. Singh, W. F. Boron, M. A. Hediger, Expression cloning of a mammalian proton-coupled oligopeptide transporter. *Nature* **368**, 563–566 (1994).
36. Y. Kanno, A. Hanada, Y. Chiba, T. Ichikawa, M. Nakazawa, M. Matsui, T. Koshiba, Y. Kamiya, M. Seo, Identification of an abscisic acid transporter by functional screening using the receptor complex as a sensor. *Proc. Natl. Acad. Sci. U.S.A.* **109**, 9653–9658 (2012).
37. S. Watanabe, N. Takahashi, Y. Kanno, H. Suzuki, Y. Aoi, N. Takeda-Kamiya, K. Toyooka, H. Kasahara, K.-i. Hayashi, M. Umeda, M. Seo, The *Arabidopsis* NRT1/PTR FAMILY protein NPF7.3/NRT1.5 is an indole-3-butyric acid transporter involved in root gravitropism. *Proc. Natl. Acad. Sci. U.S.A.* **117**, 31500–31509 (2020).
38. R. M. E. Payne, D. Xu, E. Foureau, M. I. S. T. Carquejreiro, A. Oudin, T. D. de Bernonville, V. Novak, M. Burrow, C.-E. Olsen, D. M. Jones, E. C. Tatsis, A. Pendle, B. A. Halkier, F. Geu-Flores, V. Courdavault, H. H. Nour-Eldin, S. E. O'Connor, An NPF transporter exports a central monoterpene indole alkaloid intermediate from the vacuole. *Nat. Plants* **3**, 16208 (2017).
39. C. Anne, B. Gasnier, Vesicular neurotransmitter transporters: Mechanistic aspects. *Curr. Top. Membr.* **73**, 149–174 (2014).
40. B. Lahner, J. Gong, M. Mahmoudian, E. L. Smith, K. B. Abid, E. E. Rogers, M. L. Guerinot, J. F. Harper, J. M. Ward, L. McIntyre, J. I. Schroeder, D. E. Salt, Genomic scale profiling of nutrient and trace elements in *Arabidopsis thaliana*. *Nat. Biotechnol.* **21**, 1215–1221 (2003).
41. Z.-P. Wang, H.-L. Xing, L. Dong, H.-Y. Zhang, C.-Y. Han, X.-C. Wang, Q.-J. Chen, Egg cell-specific promoter-controlled CRISPR/Cas9 efficiently generates homozygous mutants for multiple target genes in *Arabidopsis* in a single generation. *Genome Biol.* **16**, 144 (2015).
42. Y.-Q. Gao, J.-G. Chen, Z.-R. Chen, D. An, Q.-Y. Lv, M.-L. Han, Y.-L. Wang, D. E. Salt, D.-Y. Chao, A new vesicle trafficking regulator CTL1 plays a crucial role in ion homeostasis. *PLoS Biol.* **15**, e2002978 (2017).
43. D.-Y. Chao, Y. Chen, J. Chen, S. Shi, Z. Chen, C. Wang, J. M. Danku, F.-J. Zhao, D. E. Salt, Genome-wide association mapping identifies a new arsenate reductase enzyme critical for limiting arsenic accumulation in plants. *PLoS Biol.* **12**, e1002009 (2014).
44. Sunarpi, T. Horie, J. Motoda, M. Kubo, H. Yang, K. Yoda, R. Horie, W.-Y. Chan, H.-Y. Leung, K. Hattori, M. Konomi, M. Osumi, M. Yamagami, J. I. Schroeder, N. Uozumi, Enhanced salt tolerance mediated by ATHKT1 transporter-induced Na⁺ unloading from xylem vessels to xylem parenchyma cells. *Plant J.* **44**, 928–938 (2005).
45. D. G. Robinson, L. Jiang, K. Schumacher, The endosomal system of plants: Charting new and familiar territories. *Plant Physiol.* **147**, 1482–1492 (2008).
46. O. Tetyuk, U. F. Benning, S. Hoffmann-Benning, Collection and analysis of *Arabidopsis* phloem exudates using the EDTA-facilitated method. *J. Vis. Exp.*, e51111 (2013).
47. J. M. Danku, B. Lahner, E. Yakubova, D. E. Salt, Large-scale plant ionomics. *Methods Mol. Biol.* **953**, 255–276 (2013).
48. L. Cheng, F. Wang, H. Shou, F. Huang, L. Zheng, F. He, J. Li, F.-J. Zhao, D. Ueno, J. F. Ma, P. Wu, Mutation in nicotianamine aminotransferase stimulated the Fe(II) acquisition system and led to iron accumulation in rice. *Plant Physiol.* **145**, 1647–1657 (2007).
49. L. C. Crowley, B. J. Marfell, A. P. Scott, N. J. Waterhouse, Analysis of cytochrome *c* release by immunocytochemistry. *Cold Spring Harb. Protoc.* **2016**, pdb.prot087338 (2016).
50. R. Cailliatte, A. Schikora, J. F. Briat, S. Mari, C. Curie, High-affinity manganese uptake by the metal transporter NRAMP1 is essential for *Arabidopsis* growth in low manganese conditions. *Plant Cell* **22**, 904–917 (2010).
51. S. J. Clough, A. F. Bent, Floral dip: A simplified method for *Agrobacterium*-mediated transformation of *Arabidopsis thaliana*. *Plant J.* **16**, 735–743 (1998).
52. F. H. Wu, S.-C. Shen, L.-Y. Lee, S.-H. Lee, M.-T. Chan, C.-S. Lin, Tape-*Arabidopsis* sandwich–A simpler *Arabidopsis* protoplast isolation method. *Plant Methods* **5**, 16 (2009).
53. R. Tommasini, R. Evers, E. Vogt, C. Mornet, G. J. Zaman, A. H. Schinkel, P. Borst, E. Martinola, The human multidrug resistance-associated protein functionally complements the yeast cadmium resistance factor 1. *Proc. Natl. Acad. Sci. U.S.A.* **93**, 6743–6748 (1996).

Acknowledgments: We thank F. J. Zhao and D. E. Salt for critical reading of the manuscript and Y. X. He and Z. P. Zhang for the help with the microscope studies. **Funding:** This work was supported by the National Natural Science Foundation of China (31930024), Chinese Academy of Sciences (XDB27010103), Sichuan Science and Technology Program (2018HH0160), and the Newton Fund (NAF/R1\201264). **Author contributions:** D.-Y.C. and Z.-F.C. designed experiments; Z.-F.C., Y.-L.W., Y.-Y.C., C.-Y.Z., P.-Y.W., T.S., C.-B.L., Q.-Y.L., M.-L.H., S.-S.W., J.Y., and M.-G.L. performed experiments; and D.-Y.C. and Z.-F.C. wrote the manuscript. **Competing interests:** D.-Y.C., Z.-F.C., M.-L.H., Y.-L.W., P.-Y.W., and C.-Y.Z. are inventors on a pending patent related to this work filed by CAS Center for Excellence in Molecular Plant Sciences (no. 202011431787.9, filed 7 December 2020). The other authors declare that they have no competing interests. **Data and materials availability:** All data needed to evaluate the conclusions in the paper are present in the paper and/or the Supplementary Materials. Any materials described in this paper or additional data may be requested from the authors with agreement of the materials transfer agreement.

Submitted 24 February 2021

Accepted 13 July 2021

Published 3 September 2021

10.1126/sciadv.abh2450

Citation: Z.-F. Chao, Y.-L. Wang, Y.-Y. Chen, C.-Y. Zhang, P.-Y. Wang, T. Song, C.-B. Liu, Q.-Y. Lv, M.-L. Han, S.-S. Wang, J. Yan, M.-G. Lei, D.-Y. Chao, NPF transporters in synaptic-like vesicles control delivery of iron and copper to seeds. *Sci. Adv.* **7**, eabh2450 (2021).

NPF transporters in synaptic-like vesicles control delivery of iron and copper to seeds

Zhen-Fei ChaoYa-Ling WangYuan-Yuan ChenChu-Ying ZhangPeng-Yun WangTao SongChu-Bin LiuQiao-Yan LvMei-Ling HanShan-Shan WangJianbing YanMing-Guang LeiDai-Yin Chao

Sci. Adv., 7 (36), eabh2450. • DOI: 10.1126/sciadv.abh2450

View the article online

<https://www.science.org/doi/10.1126/sciadv.abh2450>

Permissions

<https://www.science.org/help/reprints-and-permissions>

Use of this article is subject to the [Terms of service](#)

Science Advances (ISSN) is published by the American Association for the Advancement of Science, 1200 New York Avenue NW, Washington, DC 20005. The title *Science Advances* is a registered trademark of AAAS.

Copyright © 2021 The Authors, some rights reserved; exclusive licensee American Association for the Advancement of Science. No claim to original U.S. Government Works. Distributed under a Creative Commons Attribution NonCommercial License 4.0 (CC BY-NC).